



Contents lists available at ScienceDirect

Environmental Technology & Innovation

journal homepage: www.elsevier.com/locate/eti

Exploring the functionality of an active ZrF-laccase biocatalyst towards tartrazine decolorization



Agnieszka Kołodziejczak-Radzimska^{a,*}, Michał Bielejewski^b,
Joanna Zembrzaska^c, Filip Ciesielczyk^a, Teofil Jesionowski^a, Long D. Nghiem^d

^a Poznan University of Technology, Faculty of Chemical Technology, Institute of Chemical Technology and Engineering, Berdychowo 4, PL-60965 Poznan, Poland

^b Institute of Molecular Physics Polish Academy of Sciences, M. Smoluchowskiego 17, PL-60179 Poznan, Poland

^c Poznan University of Technology, Faculty of Chemical Technology, Institute of Chemistry and Technical Electrochemistry, Berdychowo 4, PL-60965 Poznan, Poland

^d Centre for Technology in Water and Wastewater, School of Civil and Environmental Engineering, University of Technology, Sydney NSW 2007, Australia

ARTICLE INFO

Article history:

Received 25 March 2023

Received in revised form 28 April 2023

Accepted 9 May 2023

Available online 17 May 2023

Keywords:

Zirconia

Fucoidan

Sol-gel method

Laccase immobilization

Tartrazine decolorization

ABSTRACT

This work describes the design and fabrication of zirconia-fucoidan (ZrF) using the modified sol-gel method as the substrate for laccase immobilization (ZrF-laccase). Based on Bradford analysis, the amount of immobilized laccase and the immobilization efficiency were determined at 130 mg_{laccase}/g_{support} and 87%, respectively. The immobilization efficiency was also confirmed by determining physicochemical parameters (such as spectroscopic, thermal stability, electrokinetic, surface area and pore volume) of the prepared zirconia-fucoidan materials with and without laccase immobilization. The decrease in the value of the isoelectric point (from 6.4 to 4.0), the specific surface area (from 366 to 108 m²/g) and the pore volume (from 0.33 to 0.18 mL/g) after the immobilization process indicates effective immobilization of the laccase on the zirconia-fucoidan material. The relative activity of immobilized laccase was determined using the 2,2'-azino-bis(3-ethylbenzothiazoline-6-sulfonic acid) oxidation reaction. The ZrF-laccase biocatalytic system exhibits higher enzymatic activity than free laccase under a range of pH and temperature conditions (above 40% of initial activity) and can be reused in ten reaction cycles, retaining approximately 80% of its initial activity. The ZrF-laccase biocatalytic system was evaluated for the degradation of tartrazine as a model azo dye. The ZrF-laccase biocatalytic system could achieve 95% tartrazine decolorization in five repetitive cycles. Based on mass spectroscopy analysis, the pathway of tartrazine degradation was also proposed. Proposed methodology as well combination of zirconia, fucoidan and laccase appear to be a promising approach and open new pathways for production of highly effective biocatalyst for various applications focused on removal of emerging pollutants from the environment.

© 2023 The Authors. Published by Elsevier B.V. This is an open access article under the CC BY-NC-ND license (<http://creativecommons.org/licenses/by-nc-nd/4.0/>).

1. Introduction

Enzymatic transformation has emerged as an effective, low cost and green method for removing a range of organic contaminants from wastewater (Zdarta et al., 2021, 2022; Sai Preethi et al., 2022). Enzymes are biocatalysts that can

* Corresponding author.

E-mail address: agnieszka.kolodziejczak-radzimska@put.poznan.pl (A. Kołodziejczak-Radzimska).

accelerate the transformation of organic compounds for metabolism. They are natural molecules produced by living organisms including bacteria and fungi. Effective degradation of emerging organic contaminants including estrogens, pharmaceuticals, industrial chemicals and pesticides have been reported in the literature (Nguyen et al., 2016; Ashe et al., 2016; Morsi et al., 2020; Bilal et al., 2019). Laccases are an important enzyme that have received considerable attention in recent years due to its ability to degrade and detoxify a spectrum of dye molecules, aromatic structure and other pollutants from environmental matrices in an eco-friendly and effective manner (Aslam et al., 2022; Lou et al., 2020). The dye-based wastewater is the subject of ongoing research. Although laccases have been extensively studied to decolorize various synthetic dyes, insufficient production, poor stability, sensitivity to denaturants, lack of reusability, and high cost of purified laccase impede their industrial applications, which is why the immobilization process is a promising approach (Tišma et al., 2020; Wen et al., 2019).

As naturally produced molecules, enzymes are susceptible to degradation and suppression of enzymatic activity from harsh environmental conditions, such as extreme pH, heat, and oxidizing reagents. Thus, to increase their tolerance to environmental conditions, enzyme proteins can be immobilized onto carriers for protection (Almeida et al., 2022; Zdarta et al., 2022). The catalytic process of immobilized enzyme can increase significantly compared to free enzymes (Liu et al., 2021; Arana-Pena et al., 2021).

There are many substrates suitable for enzymatic immobilization, including activated carbon, polymers, nanomaterials and metal oxides (Araujo et al., 2022; Barhoum et al., 2022; Lopez-Cantu et al., 2022). In recent years, metal oxides, such as zirconium dioxide, have attracted significant scientific interest for enzymatic immobilization due to their thermal, chemical, and mechanical stability, high porosity, and reusability (Ibrahim and El-Desoky, 2021; Maletsky et al., 2021). Compared to organic substrates, metal oxides are less sensitive to changes in environmental conditions such as pH and temperature (Alavi et al., 2022). Zirconia-based materials have been successfully developed as substrates for enzyme immobilization (Aggarwal et al., 2021). The immobilization of lysine decarboxylase and methioninase on zirconium-based MOF materials has been reported by Yao et al. (2021) and Hassabo et al. (2019), respectively. Ahmed et al. (2018) have also successfully used Zr-based metal-organic frameworks as cellulase supports. The results of these studies showed that zirconium dioxide-based biocatalytic systems offer enhanced enzymatic activity and improved enzyme stability.

A major disadvantage of inorganic substrates, especially zirconia, is the hydrophilic nature of their surface. Without appropriate modification, it is difficult to bind enzymes to their surface and enzyme loss may occur, decreasing biocatalysts activity (Bezerra et al., 2020; Jang et al., 2021). Modification of the support surface improves biocompatibility, enabling the formation of stable bonds between the matrix and the biocatalyst. The presence of a stabilizer reduces diffusion resistance, and thus facilitates the transport of components to and from the active center of the enzyme (Aggarwal et al., 2021). Frequently used modifiers include polysaccharides, which contain at least two reactive functional groups in their structure capable of forming interactions with the support and the enzyme (Sharma et al., 2021; Wu et al., 2022).

In addition to common biopolymers, fucoidan has recently emerged as a promising modifier for the immobilization of enzymes onto zirconia. Fucoidan belongs to the group of naturally occurring sulfated polysaccharides, and can be extracted from brown algae, such as *Fucus vesiculosus* (Lahrsen et al., 2018). Fucoidan is a low-cost bioproduct, and it is also nontoxic and compatible with most biological systems. Some fucoidan-based materials have been used for medical applications (Phull et al., 2021; Matusiak et al., 2022).

Organic dyes are used in many industries, including textile manufacturing and printing. This causes high levels of pollution in water environments (Leulescu et al., 2018). Tartrazine is one of the most important azo dyes, used to produce a yellow color (Kaya et al., 2021). The areas of application of tartrazine include food products such as popsicles, ice cream, and confectionery (Gijbels et al., 2021; State et al., 2022), cosmetics such as lotions, and moisturizers (Bhattacharjee, 2020; Abu-Ghazaleh, 2022), and pharmaceuticals (Pasdaran et al., 2022). A high concentration of tartrazine can cause anxiety, hyperactivity, depression, and asthma. DNA damage and interference with DNA synthesis can occur in case of exposure to excessive amounts of tartrazine (Li et al., 2022). Some studies have shown that carcinogenic effects can also occur, resulting in subcutaneous sarcoma, liver cancer, and intestinal cancer (Munoz-Flores et al., 2022).

This article reports a novel polysaccharide-functionalized zirconia (ZrF) material synthesized via a modified sol-gel method, with fucoidan from *Fucus vesiculosus* introduced *in situ*. The key objectives of the study included: (i) preparation of a biocatalytic system based on fucoidan-functionalized zirconia and laccase; (ii) precise physicochemical characterization of obtained materials and (iii) application of enzyme-based biocatalytic system in tartrazine decolorization. Finally, the predicted mechanism as well as possible pathways of tartrazine degradation were proposed and discussed.

2. Materials and methods

2.1. Materials

Zirconium isopropoxide, isopropanol, and ammonia were used to prepare zirconia. Fucoidan from *Fucus vesiculosus* (F) was utilized as modifier and 3-aminopropyltriethoxysilane (APTES) was used as a cross-linking agent. Laccase from *Trametes versicolor* and Bradford compound were used for the immobilization process. Acetic acid and sodium acetate were used to prepare the buffer solution. The 2,2'-azino-bis(3-ethylbenzothiazoline-6-sulfonic acid) diammonium salt (ABTS) was used to determine the enzymatic activity. Tartrazine dye 85% (TT, CI 19140) was used as a model azo dye for decolorization experiment. All chemicals were of analytical grade from Sigma-Aldrich (St. Louis, MO) and were used as received without further purification.

2.2. Preparation of fucoïdan-functionalized zirconia (ZrF)

Fucoïdan-functionalized zirconia was prepared by a modified sol-gel method. First, zirconium isopropoxide was introduced into a reactor containing isopropanol, to which the ammonia solution was then added. The mixture was stirred at a speed of 1000 rpm for 1 h. Then two solutions were prepared, namely, 1 mg/mL of fucoïdan in isopropanol (1st mixture) and 1 g of APTES in isopropanol:water (4:1) (2nd mixture). Next, 20 mL of these two mixtures were simultaneously added to the reactor and continuously mixed for 30 min. The resulting sol-gel was allowed to age for 48 h, then dried at 80 °C for 24 h and finally washed with MilliQ water, filtered, and again dried (at 105 °C). Samples of the material obtained were labeled as ZrF.

2.3. Immobilization of laccase from *Trametes versicolor*

To immobilize laccase on ZrF, 0.5 g of ZrF was added to 15 mL of laccase solution (5 mg/mL, 0.2 M acetate buffer, pH = 5). Immobilization was performed in an incubator at 15 °C for 24 h. The resulting biocatalytic system was filtered under vacuum pressure and dried for 15 min at 50 °C. The immobilization efficiency was evaluated on the basis of the Bradford method. The amount of immobilized laccase (A , mg/g) and immobilization yield (IY , %) were calculated using the following Eqs. (1), (2):

$$A = \frac{(C_0 - C_1) \times V}{m} \quad (1)$$

$$IY = \frac{(C_0 - C_1)}{C_0} \times 100 \quad (2)$$

where C_0 and C_1 are the concentrations of laccase solution before and after immobilization, respectively (mg/mL), V is the volume of laccase solution (mL), and m is the mass of the ZrF support (g). The obtained biocatalytic system was labeled as ZrF-laccase. The immobilization process was performed six times and the results obtained indicate the repeatability of that process. In Table S2 (see Supplementary material), the average amount of immobilized laccase, immobilization and standard deviation were presented.

2.4. Activity assay

The 2,2'-azino-bis(3-ethylbenzothiazoline-6-sulfonic acid) (ABTS) oxidation reaction was carried out to determine the enzymatic activity of the biocatalytic system obtained under various values of the pH (2–7) and temperature (20–70 °C) of the reaction environment. In the final stage, the reusability of the biocatalytic system was determined in multiple reaction cycles (10 cycles). The oxidation reaction was performed according to the method described in our previous article (Kołodziejczak-Radzimska et al., 2021). The reactions were carried out in an incubator, at 40 °C for 20 min; next, the samples were then centrifuged and further analyzed on a Jasco V-750 UV-Vis spectrophotometer at 420 nm. All measurements were made in triplicate. Results are presented as mean \pm 3.0 SD.

2.5. Determination of kinetic parameters

The effectiveness of the immobilization process can also be studied using kinetic parameters. The immobilization process can be described using of the Michaelis-Menten constant (K_M) and the maximum reaction rate (V_{max}). These parameters were calculated for free and immobilized laccase, based on the oxidation reaction of ABTS at different concentrations (0.005–1.0 mM). The apparent kinetic parameters of the free and immobilized enzymes were calculated by using Hanes-Woolf diagrams. All measurements were made in triplicate. Results are presented as mean \pm 3.0 SD

2.6. Physicochemical evaluation

Fourier transform infrared spectroscopy (FTIR) was used to identify the functional groups present in the structures of analyzed materials. The tablets of KBr (200 mg of KBr and 1 mg of the test material) were compressed under pressure and then analyzed using a Vertex 70 analyzer (Bruker, Germany). The ^{13}C nuclear magnetic resonance spectroscopy (CP-MAS ^{13}C NMR) was employed to track the changes in the chemical structure of the investigated compounds. Analysis of high-resolution ^{13}C spectra was performed on an Avance 500 MHz spectrometer equipped with a 11.4 T superconducting magnet and a solid-state high-resolution setup (Bruker, Germany). Thermogravimetric analysis (TG/DTG) was used to evaluate the thermal stability of materials by measuring the changes in their physicochemical properties with changes in temperature. For this analysis, samples (approx. 10 mg) were heated in a temperature range of 30–1100 °C (heating rate 10 °C/min) under a nitrogen atmosphere. The evaluation was carried out using a Jupiter STA 449 F3 instrument (Netzsch, Germany). In addition, the surface area (A_{BET}) and volume (V_p) of the pores were determined using the BET (Brunauer-Emmett-Teller) and BJH (Barrett-Joyner-Halenda) algorithms. In this case, 0.3 g of the appropriate sample was degassed at 70 °C, and the analysis was carried out based on low-temperature N_2 sorption using an ASAP 2020 instrument (Micromeritics Instrument Co., USA). Due to the high precision of the instrument used, the surface area was

determined with an accuracy of $\pm 0.1 \text{ m}^2/\text{g}$ and pore volume to $\pm 0.01 \text{ mL/g}$. Furthermore, the zeta potential (ζ) and the isoelectric point (IEP) were evaluated using the ELS technique (electrophoretic light scattering) and calculated from the Henry equation. These parameters were determined using a Zeta Nano ZS instrument equipped with an automatic MPT-2 titration system (Malvern Instruments Ltd., UK). For measurement, 0.01 g of the sample was dispersed in 25 mL of 0.001 M sodium chloride solution. Titration was performed using 0.2 M HCl and NaOH solutions. The carbon, nitrogen, hydrogen, and sulfur content were evaluated to confirm the effectiveness of the preparation of ZrF hybrid material. For this purpose, the Vario EL Cube apparatus (Elementar Analysensysteme GmbH, Germany) was used. The analyzed samples (approx. 20 mg) were combusted in an oxygen atmosphere. After the gases were passed through a reduction tube, they were separated in an adsorption column and then recorded using a detector. The results are given as an average for three measurements, each accurately accurate to $\pm 0.0001\%$.

2.7. Tartrazine decolorization

Tartrazine was decolorized in the presence of a ZrF hybrid and a ZrF-laccase biocatalytic system. In this case, 100 mg of the biocatalytic system was flooded with 10 mL of tartrazine. During this process, different concentrations of tartrazine solution were used: 10, 20 and 50 mg/L. The decolorization process was analyzed with variations in time (1, 10, 30, 60, 90 and 120 min), pH (2–7), and temperature (15–75 °C). Each experiment was performed in triplicate, and the results are presented as average values. After each of these experiments, the absorbance of the resulting solution was measured at 464 nm using a V-750 spectrophotometer (Jasco, Oklahoma City, USA). The efficiency of tartrazine decolorization was calculated based on Eq. (3):

$$DE = \frac{(C_1 - C_2)}{C_1} \times 100\% \quad (3)$$

where DE is the efficiency of decolorization of TT, and C_1 and C_2 are the concentrations of tartrazine before and after the degradation process, respectively.

2.8. Mass spectroscopy (MS) analysis

Mass spectroscopy analysis was used to confirm the degradation process of tartrazine using the enzymatic method. Before analysis, the samples were diluted with methanol. Full scan ESI mass spectra were obtained on an API 4000 QTRAP mass spectrometer (AB Sciex, Foster City, CA, USA). The tartrazine dispersion was introduced into the ESI source using a syringe pump at a flow rate of 10 $\mu\text{L}/\text{min}$. The ESI operated in negative ion mode. The dye solutions were analyzed using the following settings for the ion source and mass spectrometer: curtain gas at 10 psi, nebulizer gas at 45 psi, auxiliary gas at 45 psi, temperature 400 °C. Based on the obtained MS spectra the degradation products were analyzed and possible pathway of tartrazine was proposed.

3. Results and discussion

3.1. Characterization of ZrF support and ZrF-laccase biocatalytic system

The designed zirconia-fucoidan hybrid material (ZrF) underwent several analyzes to confirm the presence of fucoidan on the ZrO_2 surface. First, the FTIR spectrum is presented in Fig. 1a. The results confirm that the ZrF hybrid contains characteristic groups raising from both zirconia and fucoidan (Supplementary material, Fig. S1). These groups include the following stretching and bending vibrations: OH (at 3450 cm^{-1}), C=O (at 1637 cm^{-1}), S=O (at 1349 cm^{-1}), C–O=S ($940\text{--}850 \text{ cm}^{-1}$), and Zr–O (below 800 cm^{-1}). These findings were also confirmed by ^{13}C -P-MAS NMR, which indicated the presence of carbonyl and sulfoxide groups, which appear at 171 and 47 ppm, respectively. Moreover, the ^{13}C -P-MAS NMR spectra for the native form of fucoidan and the ZrF hybrid (Supplementary material, Fig. S2) show qualitative changes in the chemical shifts, demonstrating the functionalization of zirconia dioxide with fucoidan.

Materials used in enzyme immobilization are required to have good thermal stability, therefore the TG/DTG curve of the zirconia-fucoidan material was determined (Fig. 1c). The ZrF material lost about 20% of its total mass, and this took place in two steps: the first at 100 °C, associated with the loss of physically adsorbed water; and the second after 200 °C, corresponding to degradation of the sulfate groups.

Because immobilization is performed by an adsorption method, the surface area of the material is especially significant. Fig. 2a shows the N_2 adsorption/desorption isotherm and the structural parameters (surface area and pore volume) of the zirconia-fucoidan material. The proposed ZrF hybrid system has a high surface area of $366 \text{ m}^2/\text{g}$ and pore volume of 0.33 mL/g , which means that this material can certainly be used as an enzyme support.

In the final step of the characterization of the ZrF hybrid, the zeta potential and isoelectric point (IEP) were determined. These parameters are important in describing the nature of surface groups of materials. The results are presented as a dependence of the zeta potential vs. pH (see Fig. 2c). The ZrF hybrid system has its IEP at pH 6.4, and its zeta potential ranges from +40 to –40 mV in the analyzed pH range. At pH 5 the surface of ZrF is positively charged, while at the same pH the surface of native laccase is negative (Supplementary materials, Fig. S3). The immobilization of laccase was carried

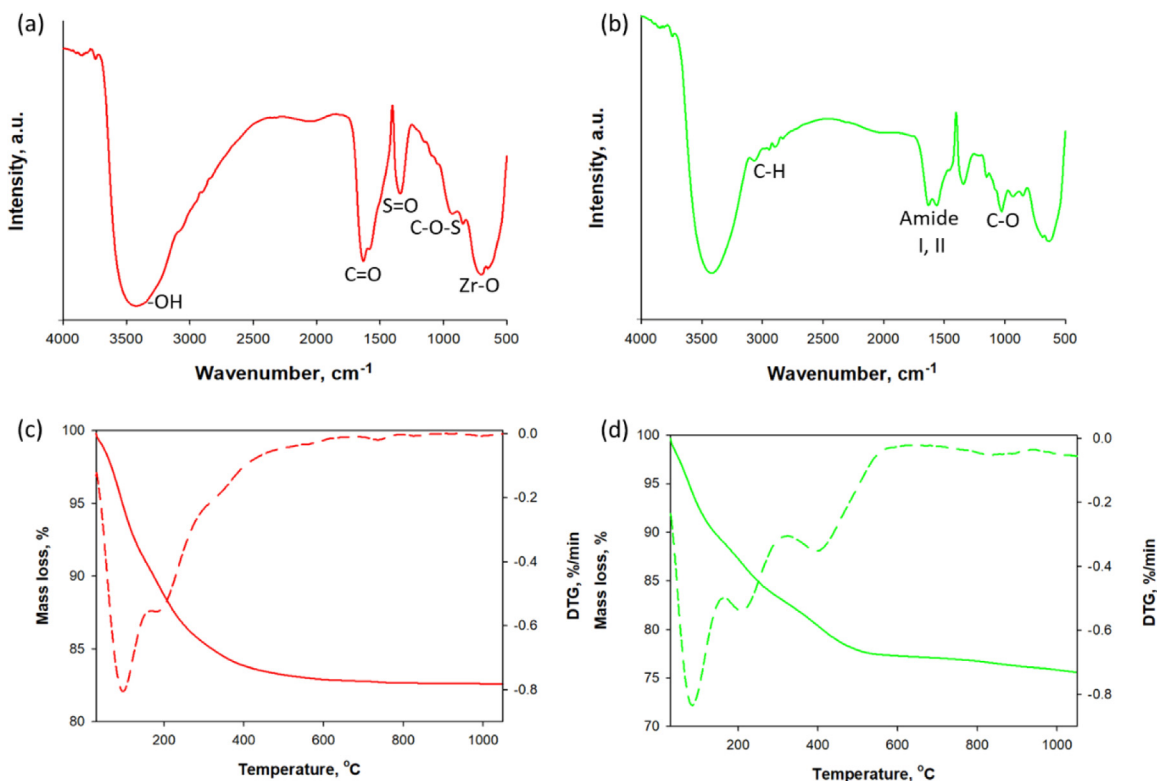


Fig. 1. FTIR spectrum of ZrF substrate (a) and ZrF-laccase system (b); thermogravimetric analysis of ZrF substrate (c) and ZrF-laccase system (d).

out at pH 5, the most favorable value for the immobilization process, and an electrostatic interaction between the enzyme and the support can be made. Furthermore, to confirm the presence of fucoidan in the zirconia structure, the content of nitrogen, carbon, and sulfur was determined (respectively 0.2%, 6.7% and 1.1%; Supplementary materials, Table S1). On the basis of the results mentioned above, it is concluded that the proposed ZrF hybrid material can serve successfully as a laccase support.

In addition, the physicochemical characteristics of the ZrF-laccase biocatalytic system were determined. The FTIR spectrum, the TG/DTG curve, N₂ adsorption/desorption isotherm, and electrokinetic curve are presented in Figs. 1 and 2. The difference between the results of the physicochemical analysis obtained before and after laccase immobilization indirectly confirms the success of this process. The FTIR spectrum (Fig. 1b) presents characteristic groups originating both, from the support (ZrF) and from laccase. The most important groups occur at the wavenumbers 2800–2900 cm⁻¹, 1400–1600 cm⁻¹, and 1050 cm⁻¹, corresponding to C–H, I and II amides, and C–O, respectively. The TG/DTG curve of ZrF-laccase (Fig. 1d) shows three steps of mass loss. The first two are the same as observed on the TG/DTG curve of the support (Fig. 1c), while the third is probably related to the decomposition of the laccase groups (Forde et al., 2010). The comparison of porous parameters (Fig. 2b) confirms that the value of surface area and pore volume decreased after laccase immobilization, which means that laccase was adsorbed on the surface as well as in the pores. Furthermore, the zeta potential decreased below pH = 6, and the isoelectric point (IEP) of the sample after laccase immobilization decreased to 4.0 (Fig. 2d). This may indicate that a single monolayer of laccase was adsorbed onto the ZrF hybrid material (Sigurdardottir et al., 2018). Based on presented results the structure of the ZrF-laccase biocatalytic system was proposed and presented in Fig. 3. The electrostatic interaction, van der Waals forces and weak hydrogen bonds can be created between enzyme and ZrF support.

3.2. Parameters of laccase immobilization

Table 1 provides an overview of the data obtained during the immobilization process. According to these data, the amount of laccase adsorbed onto the ZrF hybrid material reached 130 mg/g, which corresponds to an immobilization yield of 87%. The immobilization process was performed six times. The results obtained (Fig. 4a) indicate the repeatability of the process under the given conditions (pH 5, 15 °C, 24 h). To determine the affinity of an enzyme for its substrate, kinetic parameters such as K_M (the Michaelis–Menten constant) and V_{max} (the maximum reaction rate) were evaluated (Table 1). The measurement data produced a good fit and the kinetic parameters were easily obtained (see Supplementary

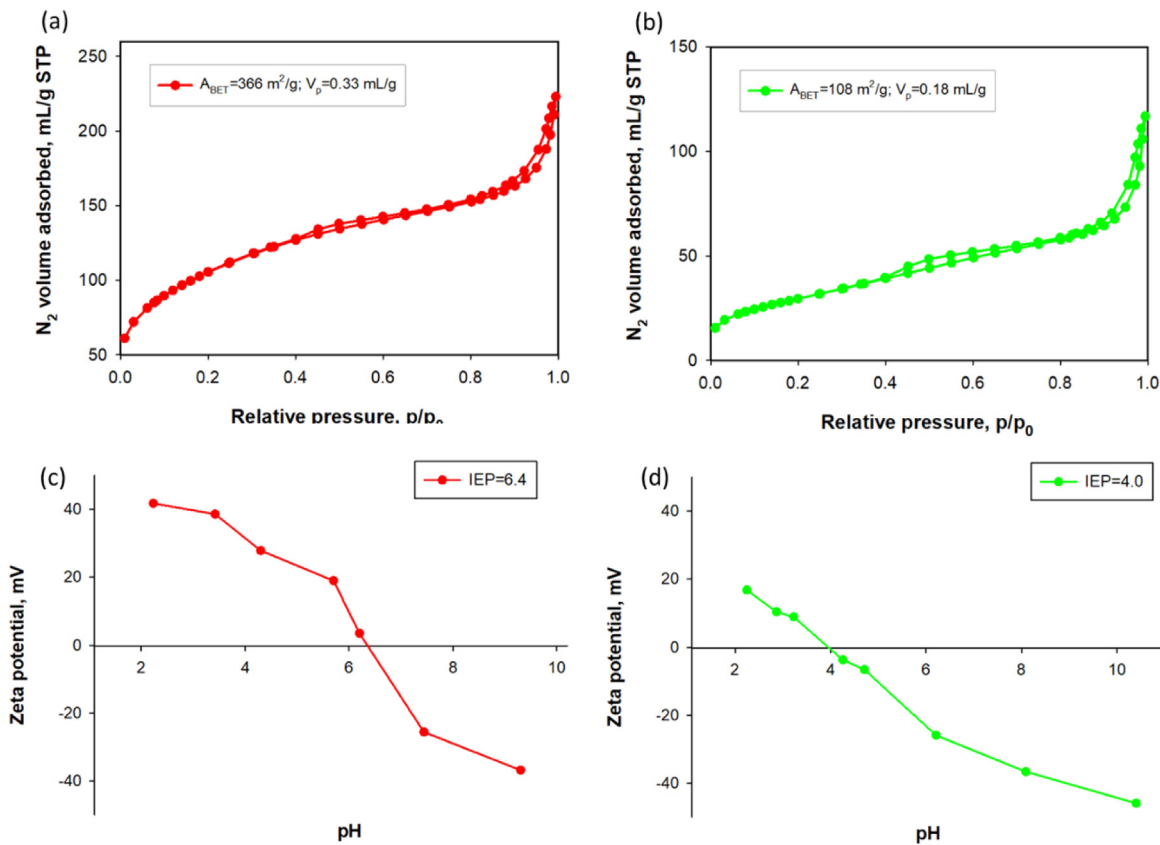


Fig. 2. N₂ adsorption/desorption isotherms of the ZrF substrate (a) and the ZrF-laccase system (b); zeta potential as a function of pH (IEP – isoelectric point) of the ZrF substrate (c) and the ZrF-laccase system (d).

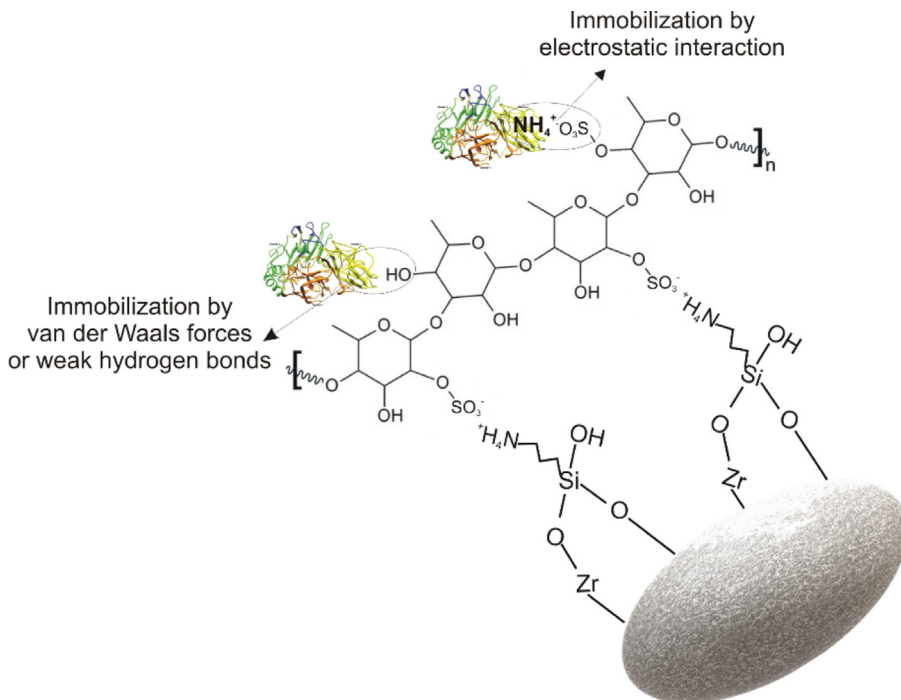


Fig. 3. The possible structure of the ZrF-laccase biocatalytic system.

Table 1
Enzymatic and kinetic parameters of native and immobilized laccase.

Sample	Enzymatic parameters		Michaelis–Menten coefficient		
	A , mg _{Lac} /g _{Support}	Y , %	K_M , mM	V_{max} , mM/min	V_{max}/K_M , min ⁻¹
Native laccase	–	–	0.18	0.027	0.149
ZrF-laccase	130 ± 4.2	87 ± 2.8	0.07	0.067	0.909

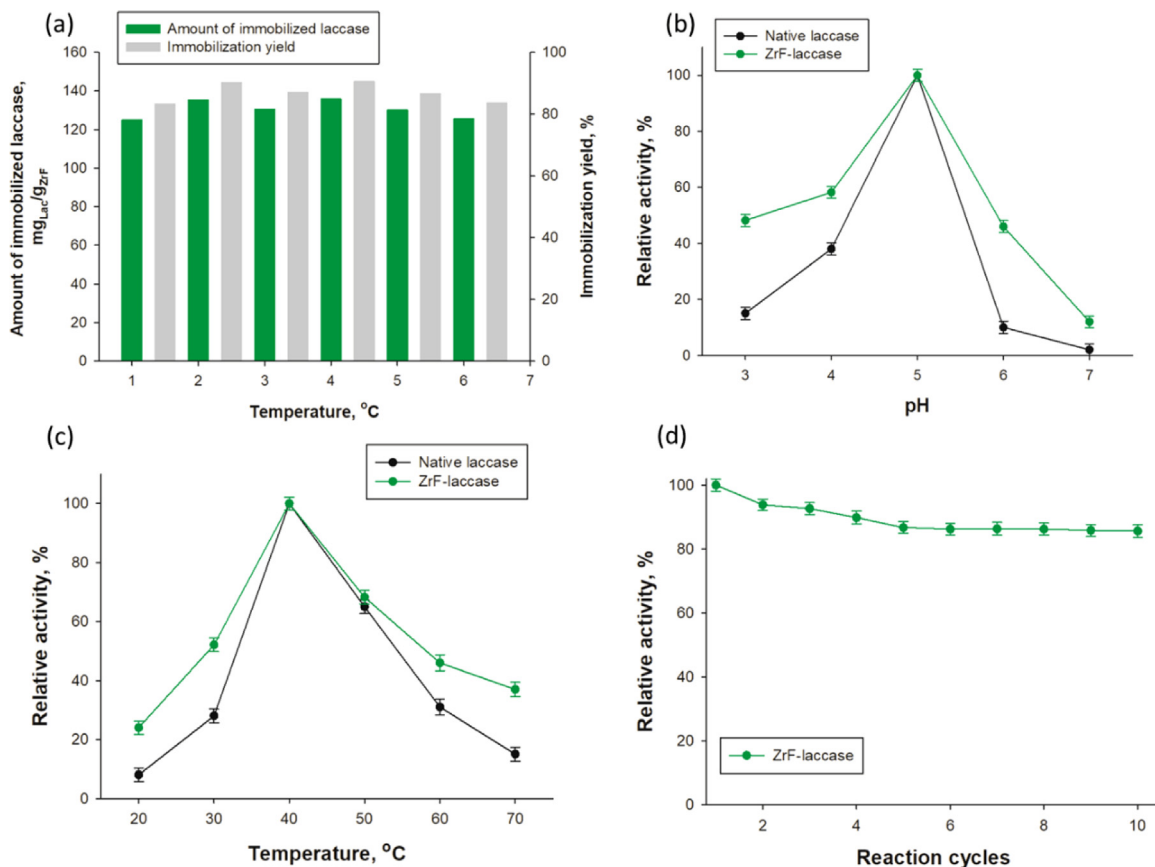


Fig. 4. Enzymatic parameters of laccase immobilization (a). Influence of pH (b) and temperature (c) on the relative activity of native and immobilized laccase (ZrF-laccase); and influence of reuse of ZrF-laccase on its enzymatic activity (d).

materials, Fig. S4). The values of these parameters indicate the affinity of the native and immobilized enzymes for the substrate, in this case, for ABTS. The K_M value of the ZrF-laccase biocatalytic system (0.07 mM) is lower than that of the native enzyme (0.18 mM), which means that the immobilized laccase has a higher affinity for ABTS than the native enzyme. The value of V_{max} increased 2.5 times (from 0.027 mM/min for native laccase to 0.067 mM/min for ZrF-laccase), indicating that the ZrF-laccase biocatalytic system can catalyze the reaction 2.5 times faster than native laccase. This is due to the reduction in the interaction between laccase and support and the reduced restriction of diffusion (Wang et al., 2022).

The influence of pH and temperature, as well as reuse over several cycles on the enzymatic activity of the designed ZrF-laccase biocatalytic system is presented in Fig. 4b–d.

The maximum enzymatic activity of both, native and immobilized laccase, occurred at pH 5 and 40 °C (Fig. 4b,c). Under conditions different from these, the relative activity decreased rapidly. However, in accordance with the expected result of immobilization, ZrF-laccase exhibited activity higher than that of the native enzyme. In the pH range between 3–6, the immobilized laccase retains approx. 40% of its initial activity. A similar result was observed in the temperature range 30–70 °C. As shown in Fig. 4d, the ZrF-laccase biocatalytic system can be used over 10 cycles, maintaining relative activity above 80%. These results show that the catalytic parameters of the designed biocatalytic system (ZrF-laccase) are superior to those of the native enzyme. The results are satisfactory as compared published so far reports in which different zirconia or biopolymer-modified materials were used in laccase immobilization (Iqhrammullah et al., 2023). Such systems as ZrO₂–Fe₃O₂ (Degórska et al., 2021), ZrO₂/cysteine (Kołodziejczak-Radzimska and Jesionowski, 2020)

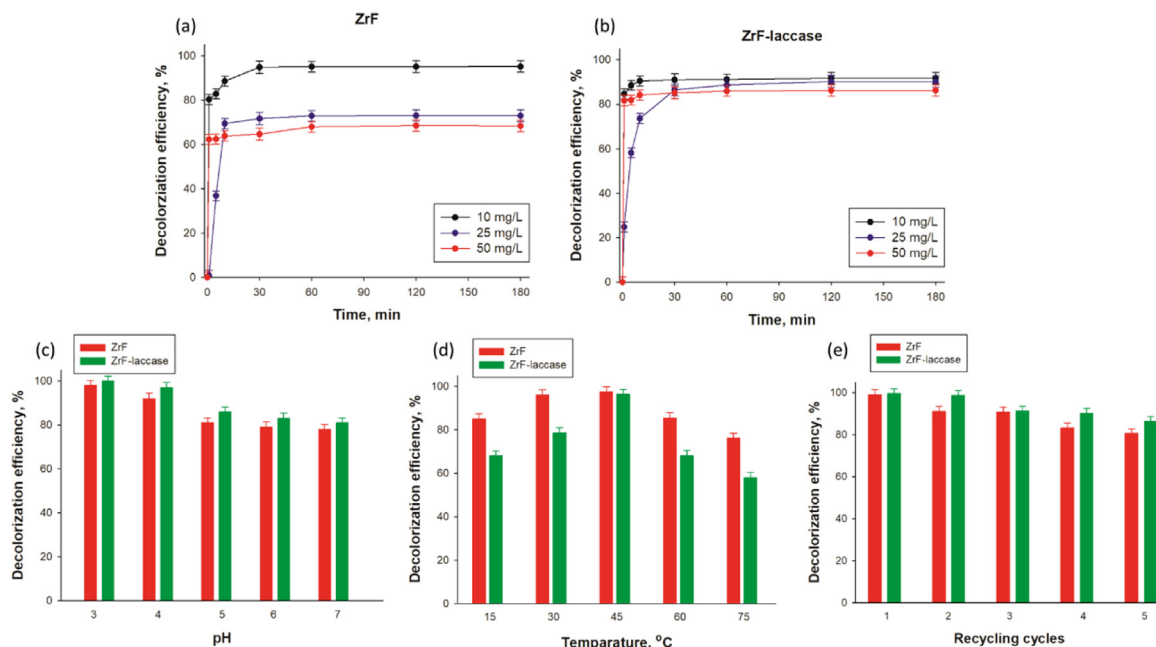


Fig. 5. Influence of time on tartrazine decolorization by the ZrF hybrid system (a) and the ZrF-laccase biocatalytic system (b). Influence of pH (c), temperature (d), and reuse cycles (e) on tartrazine decolorization by ZrF and by the ZrF-laccase biocatalytic system.

or $\text{Fe}_3\text{O}_2\text{-SiO}_2/\text{chitosan}$ (Shanmugam et al., 2020) were used as effective supports for laccase and resulted biocatalytic systems retained 80%, 70% and 80% of their initial activity after several reaction cycles, respectively.

3.3. Tartrazine decolorization

The tartrazine degradation process was performed using the ZrF hybrid and the ZrF-laccase biocatalytic system. The decolorization efficiency of tartrazine increased rapidly with reaction time and decreasing initial concentration (Fig. 5a,b). Both the ZrF hybrid and the ZrF-laccase biocatalytic system achieved more than 95% decolorization efficiency at an initial tartrazine concentration of 10 mg/L after 30 min. A significant difference was observed at higher dye concentrations. Without laccase, the decolorization efficiency decreased significantly as the tartrazine concentration increased. The decolorization efficiency by ZrF decreased to 60% as the tartrazine concentration increased to 50 mg/L. These results suggest that tartrazine decolorization by ZrF without laccase is driven by adsorption. In contrast, the tartrazine decolorization ZrF-laccase was significantly less affected by the initial tartrazine concentration. At a 50 mg/L tartrazine concentration, the decolorization efficiency only decreased slightly and was greater than 80%. Regardless of the systems used and the tartrazine concentrations, no further increase in tartrazine decolorization was observed beyond 60 min. Therefore, all subsequent decolorization experiments were conducted for 60 min.

The results indicating the influence of pH and temperature on the decolorization of tartrazine (TT) are shown in Fig. 5c,d. As evidenced, the decolorization process is affected by temperature and pH. The results presented in Fig. 5c indicate that the highest decolorization efficiency was achieved at pH 3, and as the pH increased, the value of this parameter decreased. This tendency was observed for both materials used in the decolorization process. The situation is different in the case of temperature changes. As shown in Fig. 5d, the highest decolorization efficiency was reached at 45 °C. At higher and lower temperatures, the decolorization efficiency remains high, above 80% and 60%, respectively, for ZrF and ZrF-laccase. The lower efficiency was recorded for the system with immobilized laccase than for ZrF because the laccase present on the surface is more sensitive to temperature changes. Additionally, the reduction of process costs, as an important factor in industry, was also analyzed. For that reason, the evaluation of tartrazine decolorization using the new materials based on zirconia, fucoidan, and laccase was concluded with the analysis of reusing. The results (Fig. 5e) show that both ZrF and ZrF-laccase can be used several times in the decolorization process, retaining high efficiency – even above 80% after 5 cycles.

3.4. Mass spectroscopy analysis

Mass spectroscopy analysis (MS) was used to identify the products that arise from the enzymatic degradation of tartrazine. In this case, electrospray ionization (ESI) in negative mode was used to achieve the best stability and

Table 2

Tartrazine degradation products identified by MS analysis.

Product MM, Da	Deprotonated ion MS (m/z – structure)	Ionic product MS/MS (m/z – structure)
Tartrazine, MM = 534	198 – [M–H] [–]	511 – [M–Na] [–]
A, MM = 467	467 – [M–H] [–]	449 – [M–H–H ₂ O] [–]
B, MM = 298	298 – [M–H] [–]	217 – [M–H–SO ₃ H] [–] 149 – [M–H–H] ^{2–}
C, MM = 283	283 – [M–H] [–]	269 – [M–H–N] [–]
D, MM = 239	239 – [M–H] [–]	223 – [M–H–O] [–] 157 – [M–H–C ₃ H ₂ N ₂ O] [–]
E, MM = 185	185 – [M–H] [–]	171 – [M–H–N] [–]

Table 3

Efficiency of tartrazine decolorization using different methods and materials.

Materials	Method	Decolorization efficiency	References
Carbon-containing Cu-based material	Photocatalysis	93%	Munoz-Flores et al. (2022)
TiO ₂ /g–C ₃ N ₄	Photocatalysis	93%	Cao et al. (2022)
Layered double hydroxide (LDH) [Zn ₂ –Al–Cl]	Adsorption	100%	El Khattabi et al. (2022)
Chitosan	Adsorption	95%	Dotto et al. (2012)
Laccase from <i>Streptomyces ipomoeae</i>	Enzymatic	21%	Blanquez et al. (2019)
Indigenous bacteria-acclimated microbial fuel cells (MFCs)	Biological	92%	Tacas et al. (2021)
Laccase from <i>Trametes immobilization</i>	Enzymatic	41%	This study
Laccase immobilized on ZrF hybrid material	Enzymatic	95%	This study

sensitivity of the analysis (Dos Santos et al., 2014; Popadic et al., 2021). Based on the mass spectra and m/z values obtained by MS (Supplementary material Figs. S5–S7), the possible structures were determined. The results obtained are presented in Table 2. Furthermore, the possible pathway of tartrazine degradation was shown in Fig. 6. The solutions after decolorization, at two different values of the pH = 3 and 7, were analyzed using mass spectroscopy analysis. In the MS spectra of the tartrazine solution (Fig. 4S), at both pH values (3 and 7), there is a fragment [O₃S–C₆H₄–N=C=O][–] with m/z = 198, which is characteristic of the cleavage of the pyrazalone ring. Furthermore, at pH 7, there is an ion with m/z = 467 that corresponds to the loss of three sodium ions plus the gain of two hydrogens ([M–3Na⁺2H][–]). Additionally, the presence of a hydroxylated compound is also confirmed, as a result of the loss of a water molecule (m/z = 449).

Based on the MS spectrum of the solution after degradation of TT (Figs. 5S and 6S), the following products are obtained: B (m/z = 298), C (m/z = 283), D (m/z = 239) and E (m/z = 185), the structures of which are presented in Fig. 6. The product B (m/z = 298) is obtained by cleavage of the –N=N bond, and is also present as the MS/MS ion products [B–H]^{2–} (m/z = 149) and [B–SO₃H] (m/z = 217) as a result of the loss of a sulfonic group. According to Dos Santos et al. (2014), such losses are common for polysulfonated compounds, and can be explained by the destabilization of the deprotonated ion caused by sulfate groups.

In the same way, the products C–E are identified. The ion fragment [C–N][–] (m/z = 269) is obtained by breaking the five-membered ring, and the ion [D–C₃H₂N₂O][–] (m/z = 157) is formed after the total loss of that ring. In addition, oxygen and nitrogen fragment are observed: respectively [D–O][–] (m/z = 223) and [E–N][–] (m/z = 171).

Compounds analogous to those presented above have been proposed by other researchers (Zhang et al., 2020; Dos Santos et al., 2014; Popadic et al., 2021), and confirm the possibility of the use of the prepared ZrF-laccase biocatalytic system in tartrazine degradation.

Based on reports from other researchers (Table 3) several methods and materials have been used for tartrazine decolorization. Photocatalysis is the most popular method, and has enabled tartrazine decolorization with an efficiency of 93% using the carbon–copper and titania-based material as catalysts (Munoz-Flores et al., 2022; Cao et al., 2022). Good results were also obtained by the adsorption method (95%–100%), where chitosan was used as an adsorbent (El Khattabi et al., 2022; Dotto et al., 2012). To the best of our knowledge, only free laccase has previously been used in tartrazine decolorization, but the results obtained were poorer (only 21% decolorization) (Blanquez et al., 2019). Better results were obtained when bacteria was used to tartrazine decolorization, achieving 92% efficiency (Tacas et al., 2021). In the present study, a comparison was also made between free and immobilized laccase. The results indicated that the immobilized laccase (ZrF-laccase) decolorizes tartrazine almost three times better than the free form, respectively, 95% and 41%.

4. Conclusion

Presented research demonstrates unique properties and high potential of a novel biocatalytic system of laccase immobilized onto hybrid zirconium oxide/fucoidan carrier in decolorization of azo dyes. An active hybrid carrier, based on zirconia and fucoidan, was fabricated using modified sol–gel method, efficiency of which was proved by the

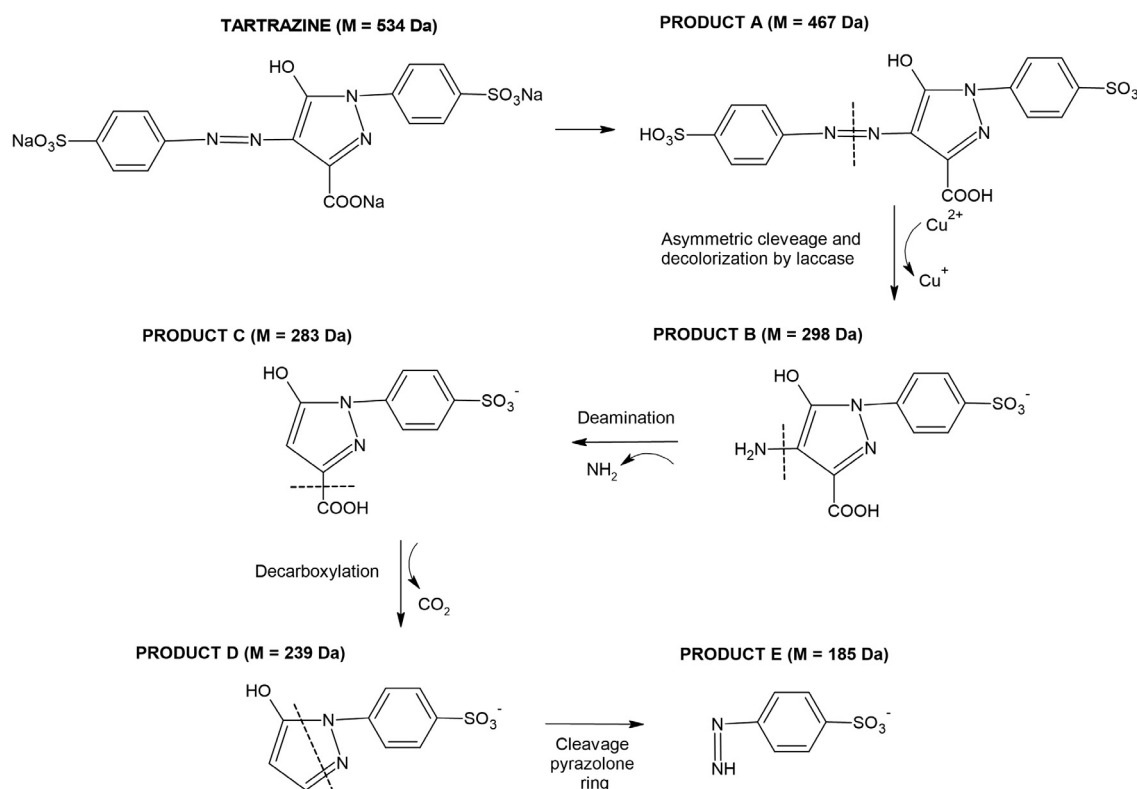


Fig. 6. Proposed pathway and mechanism of tartrazine degradation using the ZrF-laccase biocatalytic system.

physicochemical evaluation performed, including FTIR, NMR, TG/DTG, BET, elemental and electrokinetic analysis. The presence of functional groups in the ZrF hybrid (O–H, S–O), its good thermal stability, high surface area (366 m²/g) and pore volume (0.33 mL/g) qualify it as a good carrier for enzyme loading. The immobilization of laccase onto ZrF hybrid material was really efficient, as confirmed by changes in the structural parameters of the carrier (reduction of the surface area and pore volume) and electrokinetic parameters (decrease in the value of the isoelectric point) as well as the appearance of functional groups characteristic for enzyme (see FTIR spectra), which additionally suggest that electrostatic interactions, van der Waals forces and weak hydrogen bonds take part in enzyme binding with the surface of ZrF support. The designed ZrF-laccase biocatalytic system showed excellent enzymatic activity even after 10 cycles of repeated reuse, making it a potential biocatalyst for industrial applications. The key element of the research included verification tests of produced biocatalyst in tartrazine degradation. More than 95% decolorization yield of tartrazine was achieved within 60 min. Irrespectively of the process conditions (pH and temperature), which were affected by the dye concentration, the high tartrazine decolorization (under 80%) was achieved. A possible degradation pathway of the azo dye (tartrazine) was proposed together and degradation by-products were defined. Finally, it can be stated that the produced ZrF-laccase system is a promising biocatalyst because it exhibits enzymatic and kinetic parameters that predispose it for application in the removal of emerging pollutants from wastewaters.

CRedit authorship contribution statement

Agnieszka Kołodziejczak-Radzimska: Conceptualization, Data curation, Investigation, Methodology, Writing – original draft, Funding acquisition. **Michał Bielejewski:** Data curation. **Joanna Zembrzuska:** Data curation. **Filip Ciesielczyk:** Writing – review & editing. **Teofil Jesionowski:** Supervision, Writing – review & editing, Funding acquisition. **Long D. Nghiem:** Conceptualization, Investigation, Methodology, Writing – review & editing.

Declaration of competing interest

The authors declare that they have no known competing financial interests or personal relationships that could have appeared to influence the work reported in this paper.

Acknowledgments

This research was funded by the National Science Center Poland (2020/04/X/ST5/00318) and Ministry of Education and Science.

Appendix A. Supplementary data

Supplementary material related to this article can be found online at <https://doi.org/10.1016/j.eti.2023.103201>.

References

- Abu-Ghazaleh, B.M., 2022. Pretreatment with allura red or tartrazine increase resistance of *E. coli* and *Staphylococcus aureus* to some preservatives. *J. Pure Appl. Microbiol.* 16, 389–393. <http://dx.doi.org/10.22207/JPPAM.16.1.33>.
- Aggarwal, S., Chakravarty, A., Ikram, S., 2021. A comprehensive review on incredible renewable carriers as promising platforms for enzyme immobilization & thereof strategies. *Int. J. Biol. Macromol.* 17, 962–986. <http://dx.doi.org/10.1016/j.ijbiomac.2020.11.052>.
- Ahmed, I.N., Yang, X.L., Dubale, A.A., Li, R.F., Ma, Y.M., Wang, L.M., Hou, G.H., Guan, R.F., Xie, M.H., 2018. Hydrolysis of cellulose using cellulase physically immobilized on highly stable zirconium based metal-organic frameworks. *Bioresour. Technol.* 270, 377–382. <http://dx.doi.org/10.1016/j.biortech.2018.09.077>.
- Alavi, M., Kamarasu, P., McClements, D.J., Moore, M.D., 2022. Metal and metal oxide-based antiviral nanoparticles: Properties, mechanisms of action, and applications. *Adv. Colloid Interface Sci.* 306, 102726. <http://dx.doi.org/10.1016/j.cis.2022.102726>.
- Almeida, F.L.C., Prata, A.S., Forte, M.B.S., 2022. Enzyme immobilization: what have we learned in the past five years? *Biofuels. Bioprod. Bioref.* 16, 587–608. <http://dx.doi.org/10.1002/bbb.2313>.
- Arana-Pena, S., Carballares, D., Morellon-Sterling, R., Berenguer-Murcia, A., Alcántara, A.R., Rodrigues, R.C., Fernandez-Lafuente, R., 2021. Enzyme co-immobilization: Always the biocatalyst designers' choice...or not? *Biotechnol. Adv.* 51, 107584. <http://dx.doi.org/10.1016/j.biotechadv.2020.107584>.
- Araujo, R.G., Gonzalez-Gonzalez, R.B., Martinez-Ruiz, M., Coronado-Apodaca, K.G., Reyes-Pardo, H., Morreeuw, Z.P., Oyervides-Munoz, M.A., Sosa-Hernandez, J.E., Barcelo, D., Parra-Saldivar, R., Iqbal, H.M., 2022. Expanding the scope of nanobiocatalysis and nanosensing: applications of nanomaterial constructs. *ACS Omega* 7, 32863–32876. <http://dx.doi.org/10.1021/acsomega.2c03155>.
- Ashe, B., Nguyen, L.N., Hai, F.I., Lee, D.-J., van de Merwe, J.P., Leusch, F.D.L., Price, W.E., Nghiem, L.D., 2016. Impacts of redox-mediator type on trace organic contaminants degradation by laccase: degradation efficiency, laccase stability and effluent toxicity. *Int. Biodeter. Biodegr.* 113, 169–176. <http://dx.doi.org/10.1016/j.ibiod.2016.04.027>.
- Aslam, S., Ali, A., Asgher, M., Farah, N., Iqbal, H., Bilal, M., 2022. Fabrication and catalytic characterization of laccase-loaded calcium-alginate beads for enhanced degradation of dye-contaminated aqueous solutions. *Catal. Lett.* 152, 1729–1741. <http://dx.doi.org/10.1007/s10562-021-03765-8>.
- Barhoum, A., Garcia-Betancourt, M., Jeevanandam, J., Hussien, E., Mekki, S., Mostafa, M., Omran, M., Abdalla, M., Bechelany, M., 2022. Review on natural, incidental, bioinspired, and engineered nanomaterials: history, definitions, classifications, synthesis, properties, market, toxicities, risks, and regulations. *Nanomaterials* 12, 177. <http://dx.doi.org/10.3390/nano12020177>.
- Bezerra, R.M., Monteiro, R.R.C., Neto, A.D.M., da Silva, F.F.M., de Paula, R.C.M., de Lemos, T.L.G., Fechine, P.B.A., Correa, M.A., Bohne, F., Goncalves, L.R.B., dos Santos, J.C.S., 2020. A new heterofunctional support for enzyme immobilization: PEI functionalized Fe₃O₄ MNPs activated with divinyl sulfone. Application in the immobilization of lipase from *Thermomyces lanuginosus*. *Enzyme Microb. Technol.* 138, 109560. <http://dx.doi.org/10.1016/j.enzmictec.2020.109560>.
- Bhattacharjee, M., 2020. Assessment of cytotoxic potential of tartrazine (E102) on meristematic cells of vicia faba. *Pollut. Res.* 39, 1162–1167.
- Bilal, M., Iqbal, H.M., Barcelo, D., 2019. Persistence of pesticides-based contaminants in the environment and their effective degradation using laccase-assisted biocatalytic system. *Sci. Total Environ.* 695, 133896. <http://dx.doi.org/10.1016/j.scitotenv.2019.133896>.
- Blanquez, A., Rodriguez, J., Brissos, V., Mendes, S., Martins, L.O., Ball, A.S., Arias, M.E., Hernandez, M., 2019. Decolorization and detoxification of textile dyes using a versatile *Streptomyces* laccase-natural mediator system. *Saudi J. Biol. Sci.* 26, 913–920. <http://dx.doi.org/10.1016/j.sjbs.2018.05.020>.
- Cao, Y., Yuana, G., Guo, Y., Hu, X., Fang, G., Wang, S., 2022. Facile synthesis of TiO₂/g-C₃N₄ nanosheet heterojunctions for efficient photocatalytic degradation of tartrazine under simulated sunlight. *Appl. Surf. Sci.* 600, 154169. <http://dx.doi.org/10.1016/j.apsusc.2022.154169>.
- Degórska, O., Zdzarta, J., Synoradzki, K., Zgoła-Grzeszkowiak, A., Ciesielczyk, F., Jesionowski, T., 2021. From core-shell like structured zirconia/magnetite hybrid towards novel biocatalytic systems for tetracycline removal: synthesis, enzyme immobilization, degradation and toxicity study. *J. Environ. Chem. Eng.* 9, 105701. <http://dx.doi.org/10.1016/j.jece.2021.105701>.
- Dos Santos, T.C., Zaocolo, G.J., Morales, D.A., de Arago Umbuzeiro, G., Zanon, M.V., 2014. Assessment of the break down products of solar/UV induced photolytic degradation of food dye tartrazine. *Food Chem. Toxicol.* 68, 307–315. <http://dx.doi.org/10.1016/j.fct.2014.03.025>.
- Dotto, G.L., Vieira, M.L.G., Pinto, L.A.A., 2012. Kinetics and mechanism of tartrazine adsorption onto chitin and chitosan. *Ind. Eng. Chem. Res.* 51, 6862–6868. <http://dx.doi.org/10.1021/ie2030757>.
- El Khattabi, E.H., Mourid, E.H., Belaouad, S., Youssef, N., 2022. Layered double hydroxide nanomaterial as highly efficient adsorbent and its recycling after removal of a carcinogenic tartrazine dye from wastewater. *Biointerface Res. Appl. Chem.* 12, 7725–7740. <http://dx.doi.org/10.33263/BRIAC12.77257740>.
- Forde, J., Vakurov, A., Gibson, T.D., Millner, P., Whelehan, M., Marison, I.W., O'Fagain, C., 2010. Chemical modification and immobilisation of lipase b from *Candida antarctica* onto mesoporous silicates. *J. Mol. Catal. B Enzymatic* 66, 203–209. <http://dx.doi.org/10.1016/j.molcatb.2010.05.010>.
- Gijbels, E., Devisscher, L., Vinken, M., 2021. Dataset on transcriptomic profiling of cholestatic liver injury induced by food additives and a cosmetic ingredient. *Data Brief* 38, 107373. <http://dx.doi.org/10.1016/j.dib.2021.107373>.
- Hassabo, A., Mousa, A., Abdel-Gawad, H., Selim, M., Abdelhameed, R., 2019. Immobilization of L-methioninase on a zirconium-based metal-organic framework as an anticancer agent. *J. Mater. Chem. B* 7, 3268–3278. <http://dx.doi.org/10.1039/C9TB00198K>.
- Ibrahim, F.A., El-Desoky, M.M., 2021. Synthesis, structure and dielectric properties of zirconium and titanium oxide-doped lead oxide nano-crystalline films fabricated by sol-gel techniques for energy-storage application. *J. Mater. Sci. Mater. Electron.* 32, 19754–19763. <http://dx.doi.org/10.1007/s10854-021-06500-6>.
- Iqhrammullah, M., Fahrina, A., Chiari, W., Ahmad, K., Fitriani, F., Suriaini, N., Safitri, E., Puspita, K., 2023. Laccase immobilization using polymeric supports for wastewater treatment: a critical review. *Macromol. Chem. Phys.* 2200461. <http://dx.doi.org/10.1002/macp.202200461>.
- Jang, S.A., Park, J.H., Lim, H.J., Oh, J.Y., Bae, K.H., Lee, K.J., Song, J.K., Kim, D.M., 2021. Bio-specific immobilization of enzymes on electrospun PHB nanofibers. *Enzyme Microb. Technol.* 145, 109749. <http://dx.doi.org/10.1016/j.enzmictec.2021.109749>.
- Kaya, S.I., Cetinkaya, A., Ozkan, S.A., 2021. Latest advances on the nanomaterials-based electrochemical analysis of azo toxic dyes sunset yellow and tartrazine in food samples. *Food Chem. Toxicol.* 156, 112524. <http://dx.doi.org/10.1016/j.fct.2021.112524>.

- Kołodziejczak-Radzimska, A., Jesionowski, T., 2020. A novel cysteine-functionalized M_xO_y material as support for laccase immobilization and a potential application in decolorization of Alizarin red S. *Processes* 8, 885. <http://dx.doi.org/10.3390/pr8080885>.
- Kołodziejczak-Radzimska, A., Zembrzuska, J., Siwinska-Ciesielczyk, K., Jesionowski, T., 2021. Catalytic and physicochemical evaluation of a TiO_2/ZnO /laccase biocatalytic system: application in the decolorization of azo and anthraquinone dyes. *Materials* 14, 6030. <http://dx.doi.org/10.3390/ma14206030>.
- Lahrsen, E., Liewert, I., Alban, S., 2018. Gradual degradation of fucoidan from *Fucus vesiculosus* and its effect on structure, antioxidant and antiproliferative activities. *Carbohydr. Polym.* 192, 208–216. <http://dx.doi.org/10.1016/j.carbpol.2018.03.056>.
- Leulescu, M., Rotaru, A., Palarie, I., Moanta, A., Cioatera, N., Popescu, M., Morintale, E., Bubulica, M.V., Florian, G., Harabor, A., Rotaru, P., 2018. Tartrazine: physical, thermal and biophysical properties of the most widely employed synthetic yellow food-colouring azo dye. *J. Therm. Anal. Calorim.* 134, 209–231. <http://dx.doi.org/10.1007/s10973-018-7663-3>.
- Li, Q., Du, H., Li, J., Deng, J., Wang, R., Chen, Y., 2022. Sulfur-rich carbon quantum dots based on alternanthera philoxeroides and thiourea for the detection of tartrazine. *J. Mater. Sci. Mater. Electron.* 33, 12808–12818. <http://dx.doi.org/10.1007/s10854-022-08226-5>.
- Liu, S., Bilal, M., Rizwan, K., Gul, I., Rasheed, T., Iqbal, H.M.N., 2021. Smart chemistry of enzyme immobilization using various support matrices – a review. *Int. J. Biol. Macromol.* 190, 396–408. <http://dx.doi.org/10.1016/j.ijbiomac.2021.09.006>.
- Lopez-Cantu, D., González-González, R.B., Melchor-Martínez, E.M., Martínez, S.A.H., Araujo, R.G., Parra-Arroyo, L., Sosa-Hernández, J.E., Parra-Saldivar, R., Iqbal, H.M.N., 2022. Enzyme-mimicking capacities of carbon-dots nanozymes: properties, catalytic mechanism, and applications – a review. *Int. J. Biol. Macromol.* 194, 676–687. <http://dx.doi.org/10.1016/j.ijbiomac.2021.11.112>.
- Lou, C., Jing, T., Zhou, J., Tian, J., Zheng, Y., Wang, C., Zhao, Z., Lin, J., Liu, H., Zhao, C., Guo, Z., 2020. Laccase immobilized polyaniline/magnetic graphene composite electrode for detecting hydroquinone. *Int. J. Biol. Macromol.* 149, 1130–1138. <http://dx.doi.org/10.1016/j.ijbiomac.2020.01.248>.
- Maletsky, A.V., Belichko, D.R., Konstantinova, T.E., Volkova, G.K., Doroshkevich, A.S., Lyubchik, A.I., Burkhovetskiy, V.V., Aleksandrov, V.A., Mardare, D., Mita, C., Chicea, D., Khiem, L.H., 2021. Structure formation and properties of corundum ceramics based on metastable aluminium oxide doped with stabilized zirconium dioxide. *Ceram. Int.* 47, 19489–19495. <http://dx.doi.org/10.1016/j.ceramint.2021.03.286>.
- Matusiak, J., Maciołek, U., Kosinska-Pezda, M., Sternik, D., Orzeł, J., Grządka, E., 2022. Textural and thermal properties of the novel fucoidan/nano-oxides hybrid materials with cosmetic, pharmaceutical and environmental potential. *Int. J. Mol. Sci.* 23, 805. <http://dx.doi.org/10.3390/ijms23020805>.
- Morsi, R., Bilal, M., Iqbal, H.M.N., Ashraf, S.S., 2020. Laccases and peroxidases: The smart, greener and futuristic biocatalytic tools to mitigate recalcitrant emerging pollutants. *Sci. Total Environ.* 714, 136572. <http://dx.doi.org/10.1016/j.scitotenv.2020.136572>.
- Munoz-Flores, P., Poon, P.S., Ania, C.O., Matos, J., 2022. Performance of a C-containing Cu-based photocatalyst for the degradation of tartrazine: Comparison of performance in a slurry and CPC photoreactor under artificial and natural solar light. *J. Colloid Interface Sci.* 623, 646–659. <http://dx.doi.org/10.1016/j.jcis.2022.05.042>.
- Nguyen, L.N., Hai, F.I., Dosseto, A., Richardson, C., Price, W.E., Nghiem, L.D., 2016. Continuous adsorption and biotransformation of micropollutants by granular activated carbon-bound laccase in a packed-bed enzyme reactor. *Bioresour. Technol.* 210, 108–116. <http://dx.doi.org/10.1016/j.biortech.2016.01.014>.
- Pasdaran, A., Azarpira, N., Heidari, R., Nourinejad, S., Zare, M., Hamed, A., 2022. Effects of some cosmetic dyes and pigments on the proliferation of human foreskin fibroblasts and cellular oxidative stress; potential cytotoxicity of chlorophyllin and indigo carmine on fibroblasts. *J. Cosmet. Dermatol.* 9, 3979–3985. <http://dx.doi.org/10.1111/jocd.14695>.
- Phull, A.R., Ali, A., Dhong, K.R., Zia, M., Mahajan, P.G., Park, H.J., 2021. Synthesis, characterization, anticancer activity assessment and apoptosis signaling of fucoidan mediated copper oxide nanoparticles. *Arab. J. Chem.* 14, 103250. <http://dx.doi.org/10.1016/j.arabjoc.2021.103250>.
- Popadic, M.G., Marinovic, S.R., Mudrinic, T.M., Milutinovic-Nikolic, A.D., Bankovic, P.T., Dordevic, I.S., Janjic, G.V., 2021. A novel approach in revealing mechanisms and particular step predictors of pH dependent tartrazine catalytic degradation in presence of oxone[®]. *Chemosphere* 281, 130806. <http://dx.doi.org/10.1016/j.chemosphere.2021.130806>.
- Sai Preethi, P., Hariharan, N.M., Vickram, S., Rameshpathy, M., Manikandan, S., Subbaiya, R., Karmegam, N., Yadav, V., Ravindran, B., Chang, S.W., Awasthi, M.K., 2022. Advances in bioremediation of emerging contaminants from industrial wastewater by oxidoreductase enzymes. *Bioresour. Technol.* 359, 127444. <http://dx.doi.org/10.1016/j.biortech.2022.127444>.
- Shanmugam, S., Krishnaswamy, S., Chandrababu, R., Veerabagu, U., Pugazhendhi, A., Mathimani, T., 2020. Optimal immobilization of *Trichoderma asperellum* laccase on polymer coated Fe_3O_4/SiO_2 nanoparticles for enhanced biohydrogen production from delignified lignocellulosic biomass. *Fuel* 273, 117777. <http://dx.doi.org/10.1016/j.fuel.2020.117777>.
- Sharma, A., Thatai, K.S., Kuthiala, T., Singh, G., Arya, S.K., 2021. Employment of polysaccharides in enzyme immobilization. *Reactive and Functional Polymers* 167, 105005. <http://dx.doi.org/10.1016/j.reactfunctpolym.2021.105005>.
- Sigurdardottir, S.B., Lehmann, J., Ovtar, S., Grivel, J.C., Negra, M.D., Kaiser, A., Pinelo, M., 2018. Enzyme immobilization on inorganic surfaces for membrane reactor applications: mass transfer challenges, enzyme leakage and reuse of materials. *Adv. Synth. Catal.* 360, 2578–2607. <http://dx.doi.org/10.1002/adsc.201800307>.
- State, R.G., van Staden, J.K.F., State, R.N., Papa, F., 2022. Rapid and sensitive electrochemical determination of tartrazine in commercial food samples using IL/AuTiO₂/GO composite modified carbon paste electrode. *Food Chem.* 385, 132616. <http://dx.doi.org/10.1016/j.foodchem.2022.132616>.
- Tacas, A.C.J., Tsai, P.W., Tayo, L.L., Hsueh, C.C., Sun, S.Y., Chen, B.Y., 2021. Degradation and biotoxicity of azo dyes using indigenous bacteria-acclimated microbial fuel cells (MFCs). *Process Biochem.* 102, 59–71. <http://dx.doi.org/10.1016/j.procbio.2020.12.003>.
- Tišma, M., Šalić, A., Planinić, M., Zelić, B., Potočnik, M., Šelo, G., Bucić-Kojić, A., 2020. Production, characterisation and immobilization of laccase for an efficient aniline-based dye decolourization. *J. Water. Process. Eng.* 36, 101327. <http://dx.doi.org/10.1016/j.jwpe.2020.101327>.
- Wang, Z., Ren, D., Yu, H., Zhang, S., Zhang, X., Chen, W., 2022. Preparation optimization and stability comparison study of alkali-modified biochar immobilized laccase under multi-immobilization methods. *Biochem. Eng. J.* 181, 108401. <http://dx.doi.org/10.1016/j.bej.2022.108401>.
- Wen, X., Zeng, Z., Du, C., Huang, D., Zeng, G., Xiao, R., Lai, C., Xu, P., Zhang, C., Wan, J., Hu, L., Zhou, C., Deng, R., 2019. Immobilized laccase on bentonite-derived mesoporous materials for removal of tetracycline. *Chemosphere* 222, 865–871. <http://dx.doi.org/10.1016/j.chemosphere.2019.02.020>.
- Wu, T., Liu, C., Hu, X., 2022. Enzymatic synthesis, characterization and properties of the protein-polysaccharide conjugate: a review. *Food Chem.* 372, 131332. <http://dx.doi.org/10.1016/j.foodchem.2021.131332>.
- Yao, J., Lia, Z., Ji, X., Xue, Y., Ren, B., Zhao, H., Huang, Y., 2021. Novel enzyme-metal-organic framework composite for efficient cadaverine production. *Biochem. Eng. J.* 176, 10822. <http://dx.doi.org/10.1016/j.bej.2021.10822>.
- Zdarta, J., Jankowska, K., Bachosz, K., Degórska, O., Kaźmierczak, K., Nguyen, L.N., Nghiem, L.D., Jesionowski, T., 2021. Enhanced wastewater treatment by immobilized enzymes. *Curr. Pollut. Rep.* 7, 167–179. <http://dx.doi.org/10.1007/s40726-021-00183-7>.
- Zdarta, J., Jesionowski, T., Pinelo, M., Meyer, A.S., Iqbal, H.M.N., Bilal, M., Nguyen, L.N., Nghiem, L.D., 2022. Free and immobilized biocatalysts for removing micropollutants from water and wastewater: Recent progress and challenges. *Bioresour. Technol.* 344, 126201. <http://dx.doi.org/10.1016/j.biortech.2021.126201>.
- Zhang, L., Sellaoui, L., Franco, D., Dotto, G.L., Bajahazar, A., Belmabrouk, H., Bonilla-Petriciolet, A., Oliveira, M.L.S., Li, Z., 2020. Adsorption of dyes brilliant blue, sunset yellow and tartrazine from aqueous solution on chitosan: Analytical interpretation via multilayer statistical physics model. *Chem. Eng. J.* 382, 122952. <http://dx.doi.org/10.1016/j.cej.2019.122952>.